Tumor-associated macrophage-derived exosomes promote EGFR-TKI resistance in non-small cell lung cancer by regulating the AKT, ERK1/2 and STAT3 signaling pathways

SHIYANG YUAN[1*], WENJUN CHEN[2*], JIAN YANG[1], YUANHAI ZHENG[1], WEN YE[1], HUI XIE[1], LIE DONG[3] and JUNPING XIE[2]

[1]Department of Critical Care Medicine, Nanping First Hospital Affiliated to Fujian Medical University, Nanping, Fujian 353000; [2]Department of Respiratory and Critical Care Medicine, The Second Affiliated Hospital of Nanchang University, Nanchang, Jiangxi 330006; [3]Department of Respiratory and Critical Care Medicine, Nanping First Hospital Affiliated to Fujian Medical University, Nanping, Fujian 353000, P.R. China

Received March 31, 2022; Accepted July 13, 2022

DOI: 10.3892/ol.2022.13476

Abstract. The evolutionary properties of organisms lead to the issue of targeted drug resistance. Numerous clinical trials have shown that tumor-associated macrophages (TAMs) in patients with lung cancer adversely affect the clinical efficacy of epithelial growth factor receptor (EGFR) tyrosine kinase inhibitors (TKIs). However, the mechanism by which TAMs influence the tumor cell response to TKIs remains unclear. The aim of the present study was to investigate the influence of TAM-derived exosomes on the sensitivity of PC9 and HCC827 lung adenocarcinoma cells to the EGFR inhibitor gefitinib. Multiple cytokines were used to induce the differentiation of THP-1 human leukemia monocytes into macrophages *in vitro*. The obtained cells were identified as TAMs by cytomorphology and flow cytometry. Exosomes were extracted from the TAM culture supernatants and identified using electron microscopy and nanoparticle tracking analysis. Flow cytometry was used to examine the apoptosis of lung adenocarcinoma cells when treated with gefitinib and/or TAM-derived exosomes. In addition, western blotting was used to detect the expression of the key proteins of the AKT, ERK1/2 and STAT3 signaling pathways. TAM-derived exosomes were successfully obtained. The TAM-derived exosomes were shown to affect the proliferation and apoptosis of lung adenocarcinoma cells. Furthermore, the killing effect of gefitinib on the tumor cells was attenuated. The mechanism underlying the effects of the TAM-derived exosomes may be associated with reactivation of the AKT, ERK1/2 and STAT3 signaling pathways. In conclusion, the findings indicate that TAM-derived exosomes promote resistance to gefitinib in non-small cell lung cancer (NSCLC), and the mechanism may be associated with reactivation of the AKT, ERK1/2 and STAT3 signaling pathways. This study may serve as a reference in the exploration of alternative strategies for NSCLC following the development of resistance to EGFR-targeted drugs.

Correspondence to: Professor Junping Xie, Department of Respiratory and Critical Care Medicine, The Second Affiliated Hospital of Nanchang University, 1 Minde Road, Donghu, Nanchang, Jiangxi 330006, P.R. China
E-mail: junpingxie@sina.com

*Contributed equally

Key words: non-small cell lung cancer, tumor microenvironment, macrophages, gefitinib, resistance

Introduction

According to an analysis based on cancer estimates from GLOBOCAN 2020 and population estimates from the United Nations, in 2022 there will be ~4,820,000 and 2,370,000 new cases of cancer, and 3,210,000 and 640,000 cancer-associated deaths in China and the USA, respectively (1). The most common cancer in China is lung cancer, while in the USA, breast cancer is most common. However, in both China and the USA, lung cancer is the leading cause of cancer-associated mortality (1). The rapid progress of molecular genetics has brought the treatment of tumors into a new era. Non-small cell lung cancer (NSCLC) is characterized by the accumulation of changes in multiple genotypes and includes different histological subtypes. These changes in genotypes can be used as effective therapeutic targets, and a series of promising molecular inhibitors have been developed with potential in the treatment of NSCLC.

The clinical methods for the treatment of tumors are diverse, and require selection according to the clinical stage and pathological type. It is generally considered that patients with primary lung cancer can benefit from early surgery. However, there is great debate about the clinical treatment of stage III lung cancer. The American Society of Clinical Oncology guidelines (2) recommend that for patients with suspected or confirmed NSCLC, a multidisciplinary discussion should be

conducted before the initiation of treatment planning, and that patients with epithelial growth factor receptor (EGFR) 19 exon deletions or exon 21 L858R mutations may be offered adjuvant osimertinib after platinum-based chemotherapy. For the treatment of advanced NSCLC with EGFR-sensitive mutations, EGFR-targeted drug therapy is currently predominant. In the past, patients with NSCLC with other target mutations had no relevant targeted drug options and were required to undergo treatment with conventional chemotherapy regimens. In recent years, with the development of molecular medicine, targeted drugs have become available for non-EGFR mutations, including anaplastic lymphoma kinase (3), c-ros oncogene 1 (4) and MET proto-oncogene (5) mutations. To date, three generations of EGFR inhibitors have been approved by the US Food and Drug Administration for the treatment of patients with NSCLC with EGFR-activating mutations or secondary T790M mutations. Among them, the third-generation EGFR inhibitor osimertinib has attracted considerable attention. It has been reported that although patients with NSCLC with EGFR T790M mutations exhibit a positive response and prolonged survival time after treatment with osimertinib, acquired resistance also occurs after ~10 months (6). Mechanisms of third-generation EGFR inhibitor resistance have been widely explored; the C797S mutation is considered representative, and targeted drugs are under development (7). Considering the evolutionary properties of organisms, the problem of targeted drug resistance is inevitable. The continuous genetic exploration of drug resistance mechanisms and preparation of the next generation of targeted drugs is likely to be increasingly complex. Therefore, the environment on which tumor survival depends, known as the tumor microenvironment (TM), has become an alternative target of interest.

The TM is the internal environment that the tumor tissue creates and relies upon for survival and development, and has become a popular topic of tumor research. Studies have demonstrated that the TM can not only promote immune escape but also induce resistance to tumor formation (8-10). Macrophages are highly heterogeneous cells that exhibit unique phenotypes and functions in complex microenvironments within the body. Mantovani *et al* (11) suggested that macrophages exist in a series of continuous functional states, the extremes of which are type M1 and M2 macrophages. Type M1 macrophages participate in a positive immune response via the production of inflammatory cytokines and chemokines, and the presentation of antigens, while type M2 macrophages have weak antigen-presentation ability and serve an important role in immune regulation through the secretion of the inhibitory cytokines IL-10 or TGF-β. Macrophages in TM are derived from immature monocytes in the blood and formed by the microenvironment itself, where they exhibit the role and phenotype of type M2 macrophages and are known as tumor-associated macrophages (TAMs). TAMs are the major type of inflammatory cells in the tumor matrix, representing 30-50% of all inflammatory cells (12). In clinical studies, it was shown that the degree of infiltration of M2 macrophages in NSCLC tumors was positively associated with the progression of the tumor and negatively associated with the therapeutic response to EGFR-tyrosine kinase inhibitors (TKIs) (13,14). Our previous study demonstrated that TAMs induced A549 lung adenocarcinoma cells to exhibit stronger proliferation, invasion and migration capabilities via upregulation of the AKT signaling pathway (15). However, the study failed to clarify the method of communication between TAMs and lung adenocarcinoma cells. Wendler *et al* (16) hypothesized that matrix cells, fibroblasts, endothelial cells and immune cells in the TM communicate through interaction with extracellular vesicles (EVs) to jointly promote the development of tumor resistance. Exosomes are deemed to be a type of EV, with a membrane structure that mostly originates from the endometrial system and a diameter of 40-100 nm. TAMs are considered to participate in the promotion of angiogenesis of damaged tissue, cell proliferation and immune regulation (17-19). Therefore, we hypothesize that TAMs transmit proteins, factors or genetic substances through an exosome bridge, thereby affecting the sensitivity of NSCLC to EGFR-TKI drugs. However, this has not yet been confirmed by relevant research. The aim of the present study was to explore the influence of TAM-derived exosomes on the sensitivity of PC9 and HCC827 lung adenocarcinoma cells to the primary targeted drug gefitinib. The findings of the study may provide innovative ideas for delaying or blocking the process by which resistance develops.

Materials and methods

Cell culture. The THP-1 human monocytic leukemia cell line (cat. no. CL-0233) was purchased from Procell Life Science & Technology Co., Ltd. The cells were cultured in RPMI-1640 medium (Thermo Fisher Scientific, Inc.) supplemented with 10% fetal bovine serum (FBS; Gibco; Thermo Fisher Scientific, Inc.), 0.05 mM β-mercaptoethanol (Thermo Fisher Scientific, Inc.) and 1% penicillin/streptomycin (P/S; Thermo Fisher Scientific, Inc.) (100 U/ml) then incubated in a 5% CO_2 incubator at 37˚C. The PC9 (cat. no. SCSP-5085) and HCC827 (cat. no. SCSP-538) human lung adenocarcinoma cell lines were purchased from The Cell Bank of the Type Culture Collection of the Chinese Academy of Sciences. The cells were cultured in Dulbecco's modified Eagle's medium (DMEM; Thermo Fisher Scientific, Inc.) or RPMI-1640 medium supplemented with 10% FBS and 1% P/S (100 U/ml) and then incubated in a 5% CO_2 incubator at 37˚C.

Induced differentiation of THP-1 cells. THP-1 cells were treated with 100 nM phorbol 12-myristate 13-acetate (PMA; cat. no. HY-D1056) for 24 h incubated in a 5% CO_2 incubator at 37˚C, until they became adherent, indicating that the M0 phenotype had been induced. Next, using 20 ng/ml IL-4 (cat. no. HY-P70750) and 20 ng/ml IL-13 (cat. no. HY-P7033) to treat the M0 macrophages, M2 macrophages were obtained within 24 h after incubation in a 5% CO_2 incubator at 37˚C. The control group was treated with the same amount of phosphate buffered saline (PBS) at the same time point. The PMA, IL-4 and IL-13 were purchased from MedChemExpress.

Flow cytometric analysis of cellular immunophenotype and annexin V/PI staining. Cellular immunophenotyping was performed to determine the phenotypic characteristics of the cells after treatment. The processed and untreated THP-1 cells were digested with trypsin to prepare a single-cell suspension and counted to $1x10^6$ cells/ml. Next, 5.0 μl CoraLite®488 anti-human CD163 (cat. no. CL488-65169; ProteinTech Group,

Inc.) was added to 100 μl cell suspension, incubated at 2-8˚C for 30 min and washed with PBS. Finally, the cells were examined by flow cytometry (BD Accuri™ C6 Plus; BD Biosciences) and the data were processed using BD FACSDiva™ 6.1 software (BD Biosciences).

Flow cytometric analysis was also performed to detect the apoptosis characteristics of treated and untreated THP-1 cells. The cells in 6-well plates (1x10^6 cells/well) were harvested after 24 h, resuspended in PBS and then washed with PBS. Cells were stained with Annexin V (FITC)/PI (cat. no. APOAF; MilliporeSigma) according to the manufacturer's protocol. The apoptosis data were processed by flow cytometry using BD Accuri™ C6 Plus and analyzed with BD FACSDiva 6.1 software.

Extraction and identification of exosomes. The cell supernatant of the M2 macrophages was filtered using a microporous membrane (Meridian Bioscience, Inc.; pore size, 0.22 μm) and then concentrated through an Amiconultra-15 ultrafiltration tube (MilliporeSigma). After ultracentrifugation (120,000 x g, 2 h, 4˚C) the supernatant was discarded and 10 ml precooled PBS was added for resuspension and further ultracentrifugation (120,000 x g, 2 h, 4˚C). Next, the supernatant was discarded, 200 μl PBS was added for resuspension and the samples were sub-packed and frozen at -80˚C until required. The exosome protein content was measured by using a Pierce™ BCA protein assay kit (cat. no. A53226; Thermo Fisher Scientific, Inc.). To identify the exosomes, the particle sizes were examined by nanoparticle tracking analysis (NTA; ZetaView PMX 110; Particle Metrix) and the samples were characterized by transmission electron microscopy (HT-7700; Hitachi, Ltd.). The steps are as follows: Freshly separated exosomes (10 μl) were absorbed and dropped onto a copper grid with carbon-coated mesh for precipitation for 1 min. The surface water was removed with filter paper. Next, 10 μl 2 wt% aqueous uranyl acetate solution was used for positive staining at room temperature for 1 min. The surface water was removed with filter paper. Transmission electron microscopy was used after natural air drying for 10 min at room temperature to obtain images, operating at an acceleration voltage of 100 keV. In addition, the expression levels of the exosomal marker proteins CD9, CD63 and tumor susceptibility gene 101 protein (TSG101) were determined using western blotting, as described in the western blot analysis section.

Cell Counting Kit (CCK-8) assay. Different cells have different sensitivity to drugs. HCC827 and PC9 are EGFR-sensitive mutant cell lines, which are expected to be highly sensitive to gefitinib. A CCK-8 assay was used to detect the IC_{50} of gefitinib in the two cell lines. A counted cell suspension of 1x10^5 cells/ml was evenly plated into a 96-well plate, and when the cell confluence reached ~60%, 0.01, 0.03, 0.05, 0.07, 0.09, 0.11, 0.13, 0.15 and 0.17 μM gefitinib (cat. no. ZD1839; MedChemExpress) was added. After 22 h of incubation at 37˚C, 10 μl CCK-8 reagent (cat. no. CA1210; Beijing Solarbio Science & Technology Co., Ltd.) was added to each well for another 2 h. The absorbance at 450 nm was determined using a microplate reader (Thermo Fisher Scientific, Inc.). Finally, the IC_{50} of gefitinib against HCC827 and PC9 cells was calculated.

Western blot analysis. Western blotting was used for the detection of the exosomal specific marker proteins CD9, CD63 and TSG101. The protein concentrations of the THP-1 and M2 cell supernatant exosomal protein samples were determined by the bicinchoninic acid (BCA) method. Approximately 50 μg protein/lane from each sample was separated on 10% gels using SDS-PAGE electrophoresis with a 100 volt constant voltage and transferred to a PVDF membrane (GE Healthcare). Next, 5% skimmed milk powder was added to block the membrane at room temperature for 1 h. The primary antibodies, namely mouse anti-CD63 (cat. no. sc-5275; 1:500; Santa Cruz Biotechnology, Inc.), mouse anti-CD9 (cat. no. sc-13118; 1:500; Santa Cruz Biotechnology, Inc.), mouse anti-TSG101 (cat. no. sc-7964; 1:500; Santa Cruz Biotechnology, Inc.) and mouse anti-β-actin (cat. no. ab8226; 1:10,000; Abcam), were added to the membrane and incubated overnight at 4˚C. The membrane was washed with TBS with 0.1% Tween 20 (TTBS) 3 times (5 min each time), and then goat anti-mouse IgG-horseradish peroxidase (HRP) secondary antibody (cat. no. 32430; 1:5,000; Thermo Fisher Scientific, Inc.) was added for incubation at room temperature for 1 h. The film was washed 4 times with TTBS (5 min each time), SuperSignal™ West Dura Extended Duration Substrate (cat. no. 34076; Thermo Fisher Scientific, Inc.) was added dropwise, and the X-ray film was exposed in the dark for development.

The possible mechanism by which M2-derived exosomes influence the sensitivity of HCC827 and PC9 cells to gefitinib was explored. Key proteins in the AKT/ERK1/2/STAT3 signaling pathway were investigated. Gefitinib (IC_{50} concentration) and M2-derived exosomes (100 μl, 100 μg/ml) were utilized to treat HCC827 and PC9 cells separately and in combination for 24 h incubated in a 5% CO_2 incubator at 37˚C. Total protein was extracted from each group of cells and BCA was used for quantification. Protein samples (30 μg/lane) were separated on 10% gels using SDS-PAGE and transferred to PVDF membranes at 4˚C for 90 min. After blocking with 5% non-fat milk at room temperature for 60 min, membranes were incubated with the following primary antibodies overnight at 4˚C: Mouse anti-phosphorylated (p)-AKT (cat. no. 23430), mouse anti-AKT (cat. no. 2920), mouse anti-p-ERK (cat. no. 9106), mouse anti-ERK (cat. no. 4696), mouse anti-p-STAT3 (cat. no. 4113), mouse anti-STAT3 (cat. no. 9139) (all 1:1,000; Cell Signaling Technology, Inc.) and rabbit anti-GAPDH (cat. no. ab181602; 1:10,000; Abcam). The membranes were then probed with IgG HRP-conjugated goat anti-rabbit (cat. no. 32733) and goat anti-mouse (both 1:5,000; Thermo Fisher Scientific, Inc.) secondary antibodies for 1 h at room temperature. Finally, the proteins were detected using SuperSignal West Dura Extended Duration Substrate. Densitometric analysis was performed using Image J 1.44p software (National Institutes of Health).

Statistical analysis. GraphPad Prism 6 software (GraphPad Software, Inc.) was employed for statistical analysis. All data are obtained from three replicate experiments and expressed as the mean ± standard deviation (SD) of three independent experiments. Statistical differences between multiple groups were analyzed using one-way analysis of variance followed by Tukey's post hoc test. $P<0.05$ was considered to indicate a statistically significant difference.

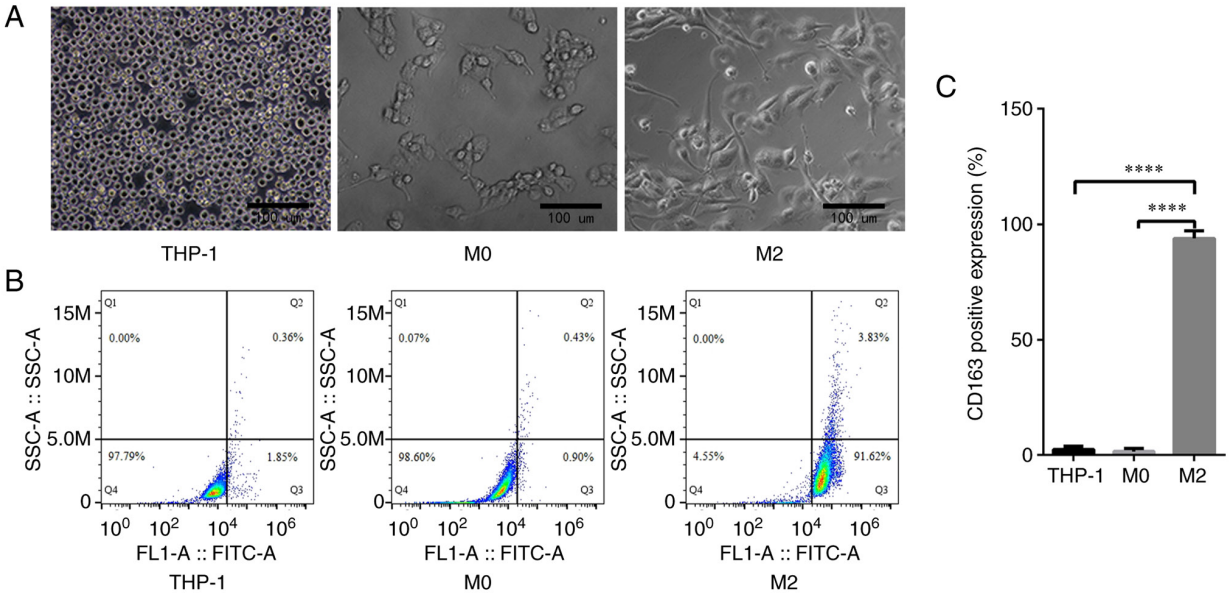

Figure 1. Formation and validation of tumor-associated macrophages. (A) Morphological changes in THP-1 cells at different stages during their induction into macrophages (magnification, x200). (B) Representative flow cytometry plots and (C) quantified CD163 expression results showing that the fluorescence intensity of CD163 in M2 macrophages was significantly higher than that in THP-1 cells and M0 macrophages. ****P<0.0001.

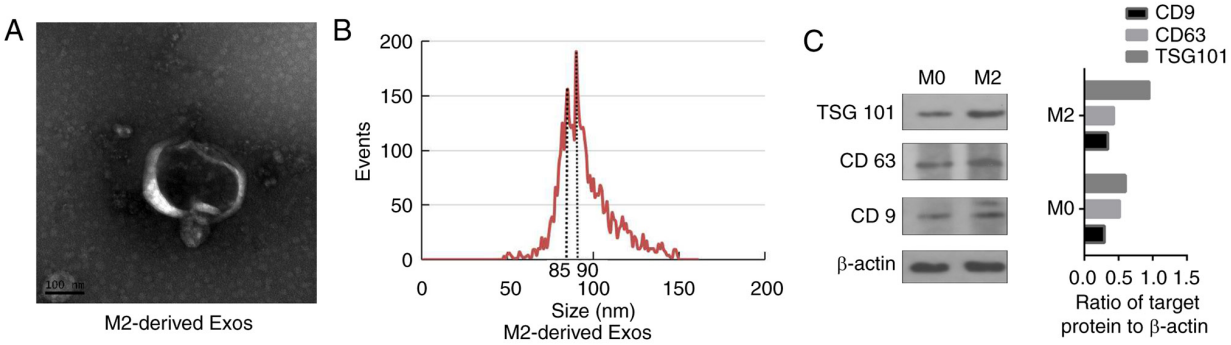

Figure 2. Identification of tumor-associated macrophage-derived exosomes. (A) The typical double-membrane vesicle structure of exosomes was clearly observed using transmission electron microscopy. (B) Nanoparticle tracking analysis showed that the diameter of the vesicle particles ranged between 50 and 150 nm, with an enrichment diameter of 90 nm. (C) Western blot analysis of exosome markers. β-actin was used as an internal control. TSG101, tumor susceptibility gene 101 protein.

Results

Formation and validation of TAMs. An inverted microscope was utilized to capture images of the THP-1 human monocytic acute leukemia cell line and the M0 and M2 macrophages derived from them. The THP-1 cells were observed to be round and grow in suspension, while the M0 macrophages were fusiform with protruding pseudopods and short antennae. However, the M2 macrophages exhibited a long fusiform or polygonal morphology with longer antennae (Fig. 1A). By incubating the THP-1 cells, M0 and M2 macrophages with CD163 antibodies and then using FACS, it was shown that the fluorescence intensity of CD163 in the M2 macrophages was significantly higher than that in the THP-1 cells and M0 macrophages (93.90±1.92 vs. 2.46±0.74 and 1.57±0.73%, respectively, P<0.0001; Fig. 1B and C).

Identification of TAM-derived exosomes. To confirm whether TAM-derived exosomes affect EGFR-TKI efficacy, exosomes were isolated from the conditioned medium of M2 macrophages by filtration and high-speed centrifugation, and were identified by electron microscopy, NTA and the detection of specific proteins. The typical double-membrane vesicle structure of the exosomes was clearly observed using electron microscopy (Fig. 2A). The NTA showed that the diameter of vesicle particles ranged between 50 and 150 nm, with an enrichment diameter of 90 nm (Fig. 2B). In addition, western blotting was used to analyze the exosome-positive markers CD9, CD63 and TSG101. The western blotting results showed that the three exosome markers were highly abundant in the extracted material (Fig. 2C). These results indicate that TAM-derived exosomes were successfully extracted.

TAM-derived exosomes affect the killing effect of gefitinib on HCC827 and PC9 cells. Different concentrations of gefitinib were applied to HCC827 and PC9 cells for 24 h. The results of the CCK-8 assay demonstrated that gefitinib had a marked dose-dependent killing effect on these two cell lines. The IC_{50} values of gefitinib against HCC827 and PC9 cells

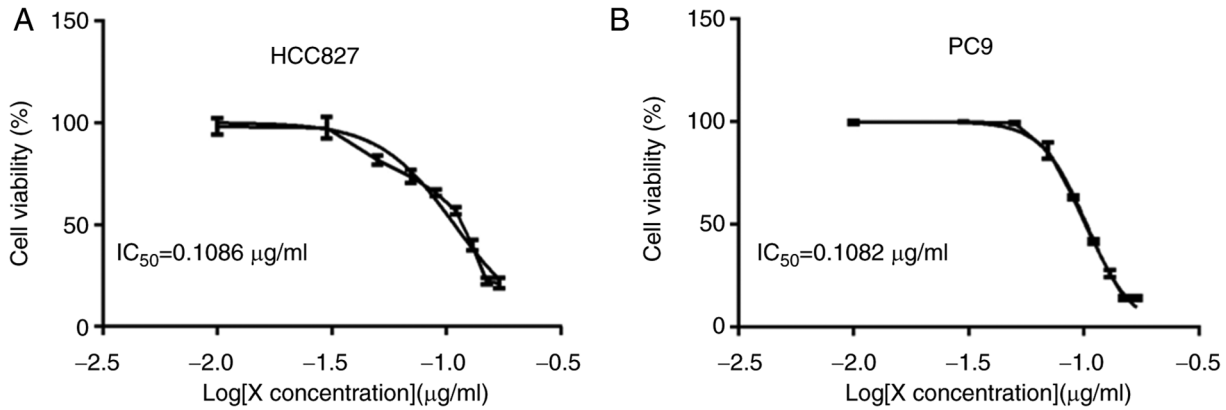

Figure 3. Killing effect of gefitinib on HCC827 and PC9 lung adenocarcinoma cells. Results of Cell Counting Kit-8 analyses showing that gefitinib had a marked dose-dependent killing effect on the (A) HCC827 and (B) PC9 cell lines.

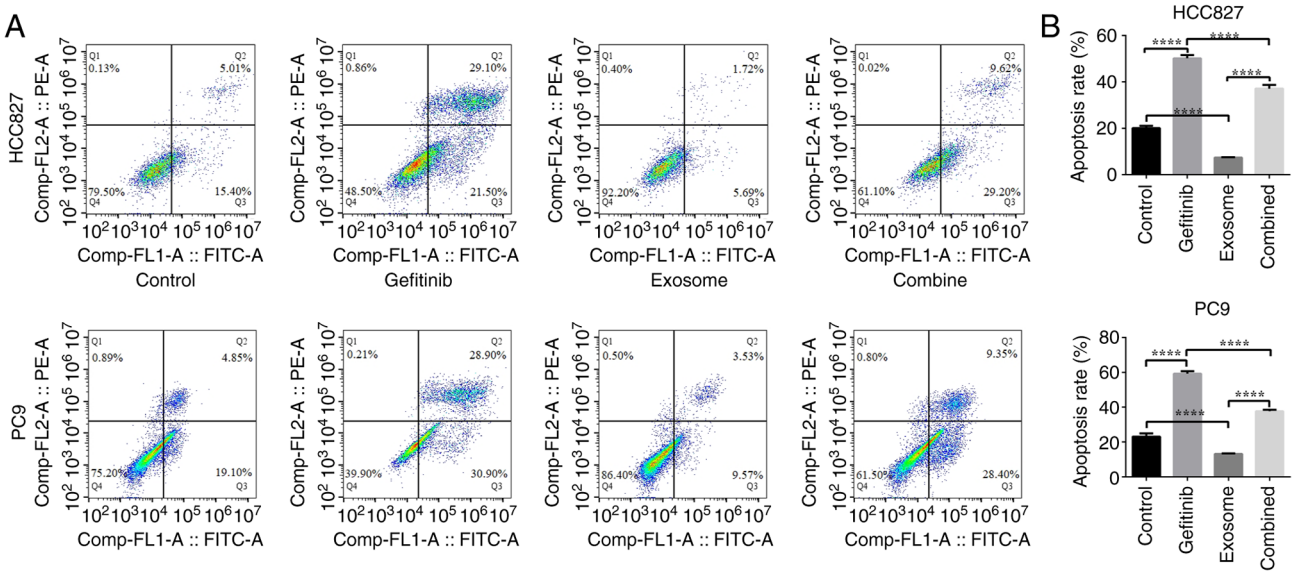

Figure 4. Exosomes derived from tumor-associated macrophages affect the apoptosis-inducing effect of gefitinib on HCC827 and PC9 cells. Effects of gefitinib and/or M2 macrophage exosomes on the apoptosis of HCC827 and PC9 cell lines were determined by flow cytometry. (A) Representative flow cytometry plots and (B) quantified apoptosis data are presented. The data indicate that gefitinib significantly induced the apoptosis of the HCC827 and PC9 cell lines, and that M2 macrophage-derived exosomes significantly reduced this effect. ****P<0.0001.

were calculated to be 0.1086 and 0.1028 μM, respectively (Fig. 3A and B). A gefitinib concentration of 0.10 μM was selected as the concentration for use in subsequent experiments.

The effects of gefitinib and M2 macrophage-derived exosomes on the early apoptosis of HCC827 and PC9 cell lines were assessed by flow cytometry. The results showed that the total apoptosis percentage in the gefitinib group was significantly increased compared with that in the blank control group (PC9: 59.21±1.52 vs. 23.12±1.82%, respectively, P<0.0001; HCC827: 50.18±1.41 vs. 20.06±1.04%, respectively, P<0.0001), and the total apoptosis percentage in the M2 macrophage-derived exosome group was reduced compared with that in the blank control group (PC9: 13.18±0.35 vs. 23.12±1.82, respectively, P<0.0001; HCC827: 7.40±0.14 vs. 20.06±1.04%, respectively; P<0.0001). The percentage of total apoptosis in the M2 macrophage-derived exosome and combination groups was significantly reduced compared with that in the gefitinib group (PC9: 13.18±0.35 and 37.66±0.80 vs. 59.21±1.52%, respectively, P<0.0001; HCC827: 7.40±0.14 and 37.14±1.57 vs. 50.18±1.41%, respectively, P<0.0001; Fig. 4A and B). These data suggest that gefitinib had a significant killing effect on the HCC827 and PC9 cell lines and that M2 macrophage-derived exosomes significantly reduced this killing effect. This prompted an exploration of the potential underlying molecular mechanism.

M2 macrophage-derived exosomes inhibit cell apoptosis by regulating the AKT/ERK1/2/STAT3 signaling pathway. Our previous research (15) explored the probable mechanism by which M2 macrophages affect the biological activity of NSCLC cells; in the present study, more possibilities were explored. Western blot analysis was used to evaluate the protein levels of AKT, p-AKT, ERK1/2, p-ERK1/2, STAT3 and p-STAT3 to verify the original hypothesis that TAMs transmit proteins, factors or genetic substances through an

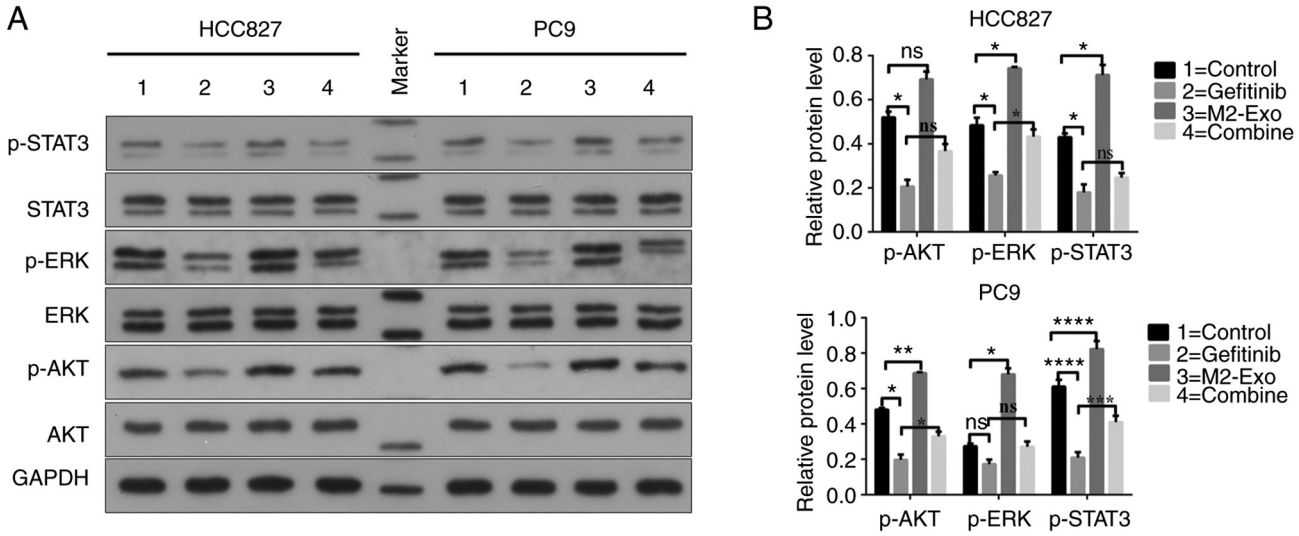

Figure 5. M2 macrophage-derived exosomes inhibit cell apoptosis by regulating the AKT/ERK1/2/STAT3 signaling pathway. Western blot analysis was used to evaluate the protein levels of AKT, p-AKT, ERK1/2, p-ERK1/2, STAT3 and p-STAT3. (A) Representative protein expression plots and (B) quantified phosphorylated target protein data are presented. In comparison with those in the control group, the levels of p-AKT, p-ERK1/2 and p-STAT3 proteins in the gefitinib group were significantly decreased. The levels of p-AKT, p-ERK1/2 and p-STAT3 in the combination group were higher than those in the gefitinib group. *P<0.05, **P<0.01, ***P<0.001 and ****P<0.0001. ns, no significant difference; p-, phosphorylated; Exo, exosome. Data are displayed as the mean ± SD.

exosome bridge, thereby affecting the sensitivity of NSCLC to EGFR-TKI drugs. The results indicated that the levels of p-AKT, p-ERK1/2 and p-STAT3 relative to their respective total proteins were markedly different between groups. Compared with the control group, the levels of p-AKT, p-ERK1/2 and p-STAT3 proteins in the gefitinib group were significantly decreased. Furthermore, the protein levels of p-AKT, p-ERK1/2 and p-STAT3 in the combination group were higher than those in the gefitinib group, although not significantly in all cases (Fig. 5A and B). These results indicate that M2 macrophage-derived exosomes attenuate the killing effect of gefitinib on HCC827 and PC9 lung adenocarcinoma cell lines by activating the AKT, ERK1/2 and STAT3 signaling pathways.

Discussion

As aforementioned, a variety of components in the TM are associated with the development of tumor drug resistance. Our previous study also demonstrated that TAMs promote the proliferation and migration of lung adenocarcinoma cells (15). Similarly, a model of TAMs was successfully established using PMA, IL-4 and IL-13 to treat the THP-1 cell line, which is a generally accepted model (20,21). There are different subtypes of macrophages. At present, M2 macrophages and TAMs are considered to serve a similar role (22), so this *in vitro* research model is academically recognized; however, M2 macrophages are not completely equivalent to TAMs, which is one of the shortcomings of the present study.

Cells can communicate with each other by cell-to-cell contact and the transmission of certain molecules. The study of EV-mediated intercellular communication is an important topic in cancer biology. Notably, tumor-derived EVs have been indicated to be involved in various processes during tumor progression, including immunosuppression and resistance to anticancer therapy (23-25). Exosomes are a type of EV with disc-shaped vesicles 40-100 nm in diameter. In the present study the extracted particles had a diameter of 50-150 nm, an enrichment diameter of 90 nm and a vesicle-like structure when observed by electron microscopy; these findings confirm that the particles were exosomes. In addition, the exosome-specific marker proteins CD9, CD63 and TSG101 were clearly detected, further confirming that M2 macrophage-derived exosomes were successfully obtained.

The results of multiple studies suggest that M2 macrophage-derived exosomes promote the proliferation of lung cancer cells and lead to antitumor drug resistance. For example, Wei *et al* (26) demonstrated that the infiltration of M2 macrophages was positively associated with the metastasis of lung adenocarcinoma, and that M2 macrophage-derived exosomes were taken up by lung adenocarcinoma cells and thereby promoted cell migration, invasion and angiogenesis. In addition, Li *et al* (27) showed that exosomes derived from M2 TAMs were able to promote cell viability, migration and invasion and the epithelial-mesenchymal transition in NSCLC, and that microRNA (miR)-155 and miR-196a-5p in exosomes served an important role in this process. Furthermore, Wang *et al* (28) demonstrated that M2 macrophage-derived exosomes are the main factor promoting cisplatin resistance in lung cancer. The mechanism was revealed to comprise the stabilization of c-Myc via the inhibition of E3 ubiquitin-protein ligase NEDD4-like, which increased the aerobic glycolysis and chemoresistance of lung cancer. By contrast, the present study explored the effect of TAM-derived exosomes on the efficacy of EGFR-targeted drugs in lung adenocarcinoma. The results suggest that TAM-derived exosomes inhibited the apoptosis of HCC827 and PC9 cells, and negatively influenced the killing effect of gefitinib; in other words, these exosomes reduce the efficacy of gefitinib. The precise mechanism may be via activation of the AKT, ERK1/2 and STAT3 signaling pathways. The present study did not include an M0-derived exosome group as a control when analyzing the mechanism,

so may have introduced some bias to the results, which is the second limitation of the paper. Also, it did not identify specific messengers or cytokines in TAM-derived exosomes, nor did it explore potential mechanisms other than the AKT signaling pathway. This the third limitation of the study and our direction of future exploration. The present study is not alone in exploring the field in which the TM leads to EGFR-TKI resistance. Zhou *et al* (29) indicated that crosstalk between cancer cells and macrophages plays a crucial role in the development of cancer. The study results suggested that NSCLC cells promote macrophage M2 polarization and suppress M1 polarization through targeting miR-627-3p/Smads signaling pathway by transferring exosomes to THP-1 cells, These changes enhanced the EGFR-TKI resistance in the NSCLC H1975 cell line. To explore alternative treatment strategies following osimertinib resistance in NSCLC, a similar study was performed by Wan *et al* (30). The results suggested that M2-type TAM-derived exosomes promoted osimertinib resistance in NSCLC by regulating the MSTRG.292666.16/miR-6386-5p/MAPK 8 interacting protein 3 axis.

In conclusion, the communication between tumor cells and other cells in the microenvironment is complex. With regard to the contribution of macrophages, tumors can recruit monocytes from the peripheral blood into the TM and then induce a transition into TAMs that promote tumor growth and mediate the development of tumor resistance. Therefore, any measure that interrupts this negative feedback loop could theoretically have an antitumor effect. The results of the present study suggest that exosomes derived from type M2 TAMs promote resistance to gefitinib in NSCLC and that the mechanism may be associated with reactivation of the AKT, ERK1/2 and STAT3 signaling pathways. The study may serve as a reference in the exploration of alternative treatment strategies for NSCLC following the development of resistance to EGFR-targeted drugs.

Acknowledgements

Not applicable.

Funding

The present study was funded by the Natural Science Foundation of Fujian Province (grant no. 2020J011312) and the National Natural Science Foundation of China (grant nos. 81160294 and 81960425).

Availability of data and materials

The datasets used and/or analyzed during this study are available from the corresponding author upon reasonable request.

Authors' contributions

SY and JX designed the study. SY, WC and HX performed the experiments. JY, YZ, WY and LD analyzed the data. SY and HX wrote the paper. SY and JX confirm the authenticity of all the raw data. All authors read and approved the final manuscript.

Ethics approval and consent to participate

Not applicable.

Patient consent for publication

Not applicable.

Competing interests

The authors declare that they have no competing interests.

References

1. Xia C, Dong X, Li H, Cao M, Sun D, He S, Yang F, Yan X, Zhang S, Li N and Chen W: Cancer statistics in China and United States, 2022: Profiles, trends, and determinants. Chin Med J (Engl) 135: 584-590, 2022.
2. Daly ME, Singh N, Ismaila N, Antonoff MB, Arenberg DA, Bradley J, David E, Detterbeck F, Fruh M, Gubens MA, *et al*: Management of stage III Non-small-cell lung cancer: ASCO guideline. J Clin Oncol 40: 1356-1384, 2022.
3. Lin JJ, Zhu VW, Schoenfeld AJ, Yeap BY, Saxena A, Ferris LA, Dagogo-Jack I, Farago AF, Taber A, Traynor A, *et al*: Brigatinib in patients with alectinib-refractory ALK-positive NSCLC. J Thorac Oncol 13: 1530-1538, 2018.
4. Peled N, Gillis R, Kilickap S, Froesch P, Orlov S, Filippova E, Demirci U, Christopoulos P, Cicin I, Basal FB, *et al*: GLASS: Global Lorlatinib for ALK(+) and ROS1(+) retrospective Study: Real world data of 123 NSCLC patients. Lung Cancer 148: 48-54, 2020.
5. Seto T, Ohashi K, Sugawara S, Nishio M, Takeda M, Aoe K, Moizumi S, Nomura S, Tajima T and Hida T: Capmatinib in Japanese patients with MET exon 14 skipping-mutated or MET-amplified advanced NSCLC: GEOMETRY mono-1 study. Cancer Sci 112: 1556-1566, 2021.
6. Schmid S, Li J and Leighl NB: Mechanisms of osimertinib resistance and emerging treatment options. Lung Cancer 147: 123-129, 2020.
7. Shaikh M, Shinde Y, Pawara R, Noolvi M, Surana S, Ahmad I and Patel H: Emerging approaches to overcome acquired drug resistance obstacles to osimertinib in non-small-cell lung cancer. J Med Chem 65: 1008-1046, 2022.
8. Ostrand-Rosenberg S: Tolerance and immune suppression in the tumor microenvironment. Cell Immunol 299: 23-29, 2016.
9. Ruffell B and Coussens LM: Macrophages and therapeutic resistance in cancer. Cancer Cell 27: 462-472, 2015.
10. Kerkar SP and Restifo NP: Cellular constituents of immune escape within the tumor microenvironment. Cancer Res 72: 3125-3130, 2012.
11. Mantovani A, Sozzani S, Locati M, Allavena P and Sica A: Macrophage polarization: Tumor-associated macrophages as a paradigm for polarized M2 mononuclear phagocytes. Trends Immunol 23: 549-555, 2002.
12. Solinas G, Germano G, Mantovani A and Allavena P: Tumor-associated macrophages (TAM) as major players of the cancer-related inflammation. J Leukoc Biol 86: 1065-1073, 2009.
13. Chung FT, Lee KY, Wang CW, Heh CC, Chan YF, Chen HW, Kuo CH, Feng PH, Lin TY, Wang CH, *et al*: Tumor-associated macrophages correlate with response to epidermal growth factor receptor-tyrosine kinase inhibitors in advanced non-small cell lung cancer. Int J Cancer 131: E227-E235, 2012.
14. Zhang B, Zhang Y, Zhao J, Wang Z, Wu T, Ou W, Wang J, Yang B, Zhao Y, Rao Z and Gao J: M2-polarized macrophages contribute to the decreased sensitivity of EGFR-TKIs treatment in patients with advanced lung adenocarcinoma. Med Oncol 31: 127, 2014.
15. Yuan S, Dong Y, Peng L, Yang M, Niu L, Liu Z and Xie J: Tumor-associated macrophages affect the biological behavior of lung adenocarcinoma A549 cells through the PI3K/AKT signaling pathway. Oncol Lett 18: 1840-1846, 2019.
16. Wendler F, Favicchio R, Simon T, Alifrangis C, Stebbing J and Giamas G: Extracellular vesicles swarm the cancer microenvironment: From tumor-stroma communication to drug intervention. Oncogene 36: 877-884, 2017.

17. Robbins PD and Morelli AE: Regulation of immune responses by extracellular vesicles. Nat Rev Immunol 14: 195-208, 2014.
18. Lee JK, Park SR, Jung BK, Jeon YK, Lee YS, Kim MK, Kim YG, Jang JY and Kim CW: Exosomes derived from mesenchymal stem cells suppress angiogenesis by down-regulating VEGF expression in breast cancer cells. PLoS One 8: e84256, 2013.
19. Looze C, Yui D, Leung L, Ingham M, Kaler M, Yao X, Wu WW, Shen RF, Daniels MP and Levine SJ: Proteomic profiling of human plasma exosomes identifies PPARgamma as an exosome-associated protein. Biochem Biophys Res Commun 378: 433-438, 2009.
20. Wu Z, Zhou J, Chen F, Yu J, Li H, Li Q and Li W: 13-Methyl-palmatrubine shows an anti-tumor role in non-small cell lung cancer via shifting M2 to M1 polarization of tumor macrophages. Int Immunopharmacol 104: 108468, 2022.
21. Sun D, Luo T, Dong P, Zhang N, Chen J, Zhang S, Dong L, Janssen H and Zhang S: M2-polarized tumor-associated macrophages promote epithelial-mesenchymal transition via activation of the AKT3/PRAS40 signaling pathway in intrahepatic cholangiocarcinoma. J Cell Biochem 121: 2828-2838, 2020.
22. Wang J, Li D, Cang H and Guo B: Crosstalk between cancer and immune cells: Role of tumor-associated macrophages in the tumor microenvironment. Cancer Med 8: 4709-4721, 2019.
23. de Goede KE, Driessen A and Van den Bossche J: Metabolic cancer-macrophage crosstalk in the tumor microenvironment. Biology (Basel) 9: 380, 2020.
24. Ruivo CF, Adem B, Silva M and Melo SA: The biology of cancer exosomes: Insights and new perspectives. Cancer Res 77: 6480-6488, 2017.
25. Pashazadeh M: The role of tumor-isolated exosomes on suppression of immune reactions and cancer progression: A systematic review. Med J Islam Repub Iran 34: 91, 2020.
26. Wei K, Ma Z, Yang F, Zhao X, Jiang W, Pan C, Li Z, Pan X, He Z, Xu J, *et al*: M2 macrophage-derived exosomes promote lung adenocarcinoma progression by delivering miR-942. Cancer Lett 526: 205-216, 2022.
27. Li X, Chen Z, Ni Y, Bian C, Huang J, Chen L, Xie X and Wang J: Tumor-associated macrophages secret exosomal miR-155 and miR-196a-5p to promote metastasis of non-small-cell lung cancer. Transl Lung Cancer Res 10: 1338-1354, 2021.
28. Wang H, Wang L, Pan H, Wang Y, Shi M, Yu H, Wang C, Pan X and Chen Z: Exosomes derived from macrophages enhance aerobic glycolysis and Chemoresistance in lung cancer by stabilizing c-Myc via the inhibition of NEDD4L. Front Cell Dev Biol 8: 620603, 2020.
29. Zhou D, Xia Z, Xie M, Gao Y, Yu Q and He B: Exosomal long non-coding RNA SOX2 overlapping transcript enhances the resistance to EGFR-TKIs in non-small cell lung cancer cell line H1975. Hum Cell 34: 1478-1489, 2021.
30. Wang J, Li D, Cang H and Guo B: Crosstalk between cancer and immune cells: Role of tumor-associated macrophages in the tumor microenvironment. Cancer Med 8: 4709-4721, 2019.